# ELEMENTARY THEORY OF ASSOCIATIONS BETWEEN ATMOSPHERIC MOTIONS AND DISTRIBUTIONS OF WATER CONTENT[1]

EDWIN KESSLER, III

The Travelers Research Center, Inc., Hartford, Conn.

[Manuscript received August 2, 1962; revised October 24, 1962]

## ABSTRACT

Continuity equations are used to clarify relationships between air motions and distributions of accompanying precipitation. The equations embody simple modeling of condensation and evaporation with the following assumptions: (1) water vapor shares the motion of the air in all respects; (2) condensate shares horizontal air motion, but falls relative to air at a speed that is the same for all the particles comprising precipitation at a particular time and height; (3) the cloud phase is omitted.

After a review of one-dimensional models, the distributions of condensate in two-dimensional model wind fields are discussed with regard to instantaneous evaporation of condensate in unsaturated air and to no evaporation. The most nearly natural cases must lie between these extremes. The methods for obtaining solutions are instructive of basic interactions between air motion and water transport. The steady-state precipitation rate from a saturated horizontally uniform updraft column is shown to equal the sum of the vertically integrated condensation rate and a term that contains the horizontal divergence of wind. The latter term becomes relatively small as the ratio of precipitation fall speeds to updrafts becomes large. A basis for some studies of precipitation mechanisms, the equation $N(V+w)=$const., where $N$ is the number of particles comprising precipitation at a particular point in space and time, $V$ is their fall velocity, and $w$ is the updraft, is shown to imply violation of continuity principles unless variations in $w$ are quite small. Continuity equations are applied to radar-observed convective cells (generators) and their precipitation trails, and to radar-observed precipitation pendants (stalactites), and provide bases for estimating the strength, duration, and vertical extent of the associated vertical air currents. The stalactite study also discloses how horizontal variations of precipitation intensity arise during precipitation descent through a saturated turbulent atmosphere.

The continuity equations are powerful tools for illuminating fundamental properties of wind-water relationships. The conclusion discusses attractive paths along which this work should be extended.

## 1. INTRODUCTION

The study of time-dependent relationships between wind fields and water distributions derives from the belief that knowledge of wind-water relationships is essential for an intelligent approach to the numerous hydrometeorological problems which hold the increasing direct interest of mankind. Use of wind-water relationships in meteorological analysis should assist the interpretation of radar and satellite observations. Knowledge of the relationships between wind and water fields should assist our consideration of means to modify the weather, since the distributions of water are interwoven with the distributions of latent and sensible heat and the scale, intensity, and shape of convective processes.

This report discusses the application of continuity equations to several interesting problems. Some previously published material (Kessler [4] and [5], and Kessler and Atlas [6]), is briefly reviewed to give coherence to this paper, but the emphasis here is on previously unpublished work.

The principal assumptions have been: (1) Water vapor shares the motion of the air in all respects. (2) Condensate shares the horizontal motion of the air but falls relative to the air at a speed $V$. $V$ is a negative parameter that may vary with height but that is constant with time at any given height. (This is a great simplification of cloud physics processes—precipitation having a fall velocity $V$ is assumed to form as the result of condensation without a cloud phase. At any particular height, all of the precipitation particles fall at the same speed.) (3) The moisture capacity of the air is a function of height only. (4) The air density is considered locally steady and horizontally uniform.

These premises lead to a continuity equation for $M$, the density of water substance in all its phases minus the saturation vapor density, viz.,

$$\frac{\partial M}{\partial t}=-u\frac{\partial M}{\partial x}-v\frac{\partial M}{\partial y}-w\left(\frac{\partial M}{\partial z}-G\right)-\frac{\partial}{\partial z}(MV)+Mw\frac{\partial \ln \rho}{\partial z} \quad (1)$$

[1] Most of the work reported here was substantially completed while the author was employed at the Weather Radar Branch, Geophysics Research Directorate, Air Force Cambridge Research Laboratories. The preparation of this paper has been supported by the U.S. Army Electronics Research and Development Laboratories under Contract DA 36-039 SC 89099. The results given in Sections 6 and 7 were first presented at the Ninth Weather Radar Conference at Kansas City, Mo., in October 1961, and were printed in the *Proceedings* of that conference.

where $u$ and $v$ are the winds in the $x$ and $y$ (horizontal) directions, $w$ is the wind in the $z$ (vertical) direction, and $\rho$ is the air density. $G$ is a generation term that denotes the amount of water condensed from a unit volume of saturated air for each unit vertical distance of air travel; $G=-\rho(dQ/dz)$, where $Q$ is the saturation mixing ratio of water vapor in air (for derivation of equation (1), see [4] Section 2).[2]

When $M$ is negative, it shares the motion of the air and represents the amount of moisture that must be added to saturate the air; when $M$ is positive, it falls relative to the air at a speed $V$, and represents the amount of condensate in saturated air. $Q$ plus $M$ is the total water content. These associations between $M$ and $V$ imply instantaneous evaporation of condensate in unsaturated air, a fact clearly perceived when one considers that the term $MV=0$ wherever $M<0$. The descent of condensate contributes at a rate $MV$ to the addition of $M$ in unsaturated air just beneath, the rate of addition being unaffected by the magnitude of $M$ in the drier air until $M>0$. Only when $M>0$ can there be a fallout of water substance.

By treating condensate and vapor separately in two equations, it is practical to study the situation in which precipitation once formed does not evaporate in subsaturated air. This is discussed further in section 5b below.

## 2. THE DISTRIBUTION OF $M$ ALONG VERTICALS WHERE THERE IS NO HORIZONTAL ADVECTION

This section summarizes results presented in several other places, and is included here to facilitate understanding of the new results presented in following sections.

### A. $V+w$ EVERYWHERE LESS THAN ZERO (MOTION OF CONDENSATE EVERYWHERE DOWNWARD)

(1) *Steady state solutions.*

Omission of compressibility simplifies the discussion without affecting the principal conclusions, and the following expression for the distributions of $M$ in time and height is therefore considered.

$$\frac{\partial M}{\partial t}=-(w+V)\frac{\partial M}{\partial z}-M\frac{\partial V}{\partial z}+wG. \qquad (2)$$

When $V$ is everywhere the same, a condition most closely approached in snow, the third term in equation (2) is zero. The steady-state vertical profile of $M$ in a saturated atmosphere is then given by

$$M(z)=M(H)+\int_H^z\left(\frac{wG}{w+V}\right)dz. \qquad (3)$$

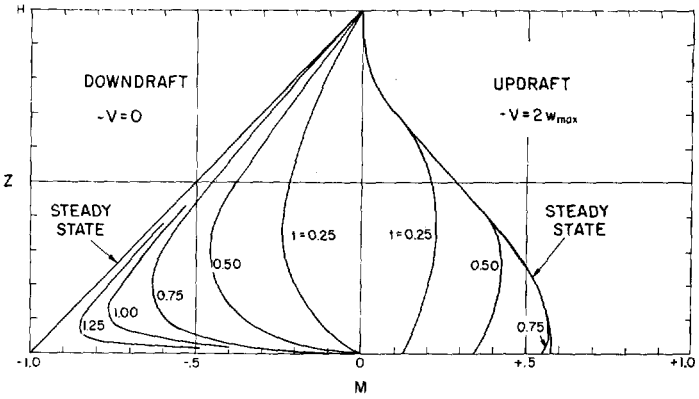


FIGURE 1.—One-dimensional time-dependent and steady $M$-distributions in downdrafts (left) and updrafts (right), when $G$ is constant. Values on the abscissa refer to the total water content minus the saturation vapor content in gm./m.$^3$ when $H=1$ km. and $G=1$ gm. m.$^{-3}$ km.$^{-1}$ Vertical velocity $w=(4\ w_{max}/H)\times[z-(z^2/H)]$.

This integral has been evaluated exactly for several values of $V$ and a parabolic vertical distribution of updraft $w$, with $w=0$ at $z=0$, $H$. A typical result with $M(H)=0$ is shown in the right side of figure 1, taken from [5]. A discussion of the application of (3) to the descent of condensate in saturated downdrafts is given toward the close of section 7.

When $V=0$, the steady-state solutions are independent of the shape of the updraft distribution. Equation (3) then gives, for updrafts, the limiting form of the distribution approached after a very long time with the unrealistic condition that condensate indefinitely retains negligible falling speed. The application to downdrafts of equations (2) and (3) with $V=0$ has a fairly reasonable basis; the solution there represents the distribution of saturation deficit attained after sinking motion has continued for a very long time. This solution for constant $G$ is illustrated in the left side of figure 1.

When $V$ is variable, the third term in (2) must be retained and this equation's steady-state form is then not readily solved analytically. In such cases, finite difference approximations have been used to obtain the solutions. Figure 2 shows computed steady-state profiles of $M$ in the model snowstorm situation indicated by table 1. These profiles suggest that some of the upper layers observed by radar in winter storms may be due to the kinematic principles discussed here, rather than to the widely discussed generator and trail mechanism (Marshall [10], for example), which, it is agreed, is the significant factor in most such observations. Since increases of fall velocity are generally associated with increases in particle diameter (to whose sixth power radar is sensitive), a layer of enhanced radar reflectivity is not likely to accompany a layer of enhanced water content that is due to the divergence of precipitation fall velocities. This and several

[2] When $M$ and $G$ are in mixing ratio units, equation (1) is the same except that the last term becomes $-MV(\partial\ln\rho/\partial z)$, and $G=-dQ/dz$. Density units are used in this study because radar reflectivity characteristics, visual appearance, and certain physical effects are best understood in such terms.

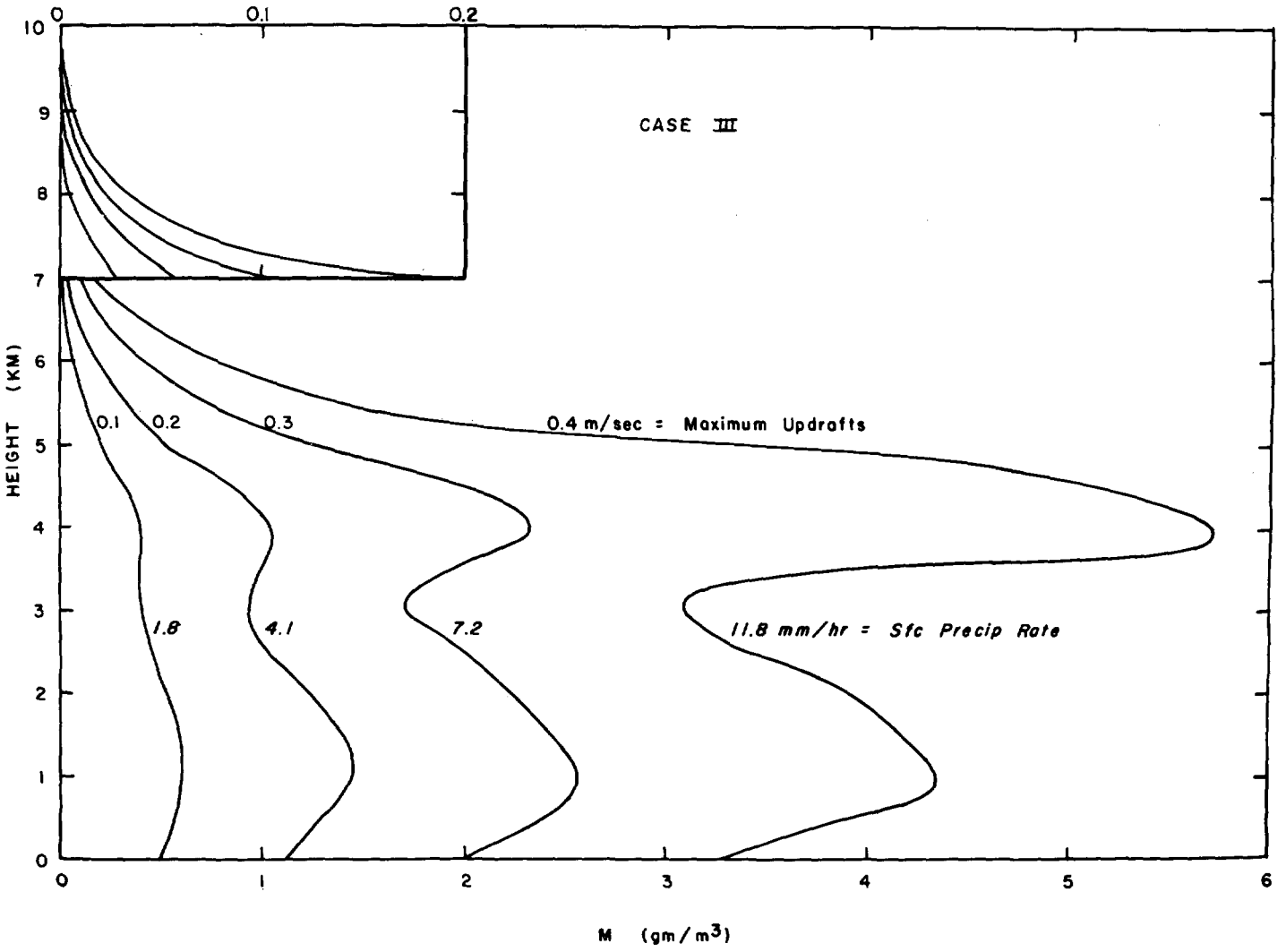


FIGURE 2.—Theoretical steady-state water-content profiles for various surface snowfall rates near the precipitation center of a winter storm. The maxima occur above layers in which the particles increase their fall speed during descent. The profiles have been calculated using the parameter distributions given in table 1. (From [6].)

other steady-state variable-$V$ cases have been treated elsewhere (Kessler and Atlas [6]).

TABLE 1.—*Abbreviated tabulation of model atmosphere parameters used to compute the profiles of figure 2*

| Height (km.) | Approximate pressure (mb.) | Relative updraft $w$ | $T$ (° C.) | $G\times10^4$ (gm./m.$^4$) | Particle fall speed (cm./sec.)[1] |
|---|---|---|---|---|---|
| 0 | 1015 | 0 | 0 | 16.8 | 100 |
| 1 | 900 | 36 | −7 | 12.3 | 75 |
| 2 | 795 | 64 | −6 | 12.0 | 75 |
| 3 | 700 | 84 | −4 | 12.6 | 75 |
| 4 | 615 | 96 | −9 | 9.7 | 50 |
| 5 | 540 | 100 | −17 | 6.4 | 50 |
| 6 | 470 | 96 | −26 | 3.9 | 50 |
| 7 | 410 | 84 | −35 | 1.9 | 50 |
| 8 | 355 | 64 | −43 | 0.8 | 50 |
| 9 | 310 | 36 | −50 | 0.4 | 50 |
| 10 | 265 | 0 | −53 | 0.3 | 50 |

[1] 50 cm./sec. used where $T<-8°$ C.; where temperature increases above −8° C. following the descent of $M$, the speed is taken as a linear increase with temperature to 100 cm./sec. at 0° C.

667117—63——3

(2) *Time-dependent solutions*

In the steady cases, the vertical distribution of $M$ depicts the individual changes following the descent of $M$; i.e., $dM/dz=\partial M/\partial z$. When $\partial V/\partial z=0$, $dM/dz$ is independent of $M$, and the steady-state profiles provide the key to easy determination of the time-dependent solutions. The packets of $M$ change by an amount $dM=(\partial M/\partial z)\,dz$ while descending through $dz$ in a time $dt=dz/(V+w)$. The time-dependent solutions when $V$ is invariant can, therefore, be constructed from the steady-state vertical profile of $M$ and the curve showing the height of an $M$-packet against time. Two sets of results of such calculations based on the initial condition $M\equiv0$ and the upper boundary condition $M(H)=0$ are illustrated in figure 1 and are discussed in detail in [4] and [5]. When the fall velocity is a function of height, this method of solving for the time-dependent solutions is inadequate, but it is practical in such cases to use finite difference methods.

Many properties of the variable-$V$ solutions can be qualitatively assessed from general considerations supplemented by simple computations.

### B. $V+w$ SOMEWHERE GREATER THAN ZERO (MOTION OF CONDENSATE SOMEWHERE UPWARD)

With $V$ constant and the absolute magnitude of $V$ anywhere less than the associated value of $w$, there is no steady-state solution valid throughout the depth of the updraft column. However, in this case, where $V$ is everywhere the same, the time-dependent solutions at points where $(V+w)=0$ are simply $M=M_0+wGt$, and elsewhere can be accurately determined by a procedure only slightly more elaborate than that described above for determining the time-dependent solutions that precede a steady state. (See [5], Sec. 4.)

## 3. THE STEADY-STATE PRECIPITATION RATE FROM A SATURATED, HORIZONTALLY UNIFORM UPDRAFT COLUMN

The application of continuity considerations shows that the rate of steady precipitation at the ground is not generally equal to the condensation rate in rising air vertically above, even when there is no horizontal advection at the center of an area of widespread updrafts. Equality of steady precipitation and condensation rates is approached as the magnitude of the ratio of precipitation fall speeds to updrafts increases. The results presented here are an extension of section 5 in [4].

In a steady-state horizontally uniform atmosphere, the horizontal advection terms are zero and the appropriate equation is:

$$0=-w\frac{\partial M}{\partial z}-\frac{\partial}{\partial z}(MV)+wG+Mw\frac{\partial \ln \rho}{\partial z} \tag{4}$$

Integration from the base 0 to the top $H$ of the updraft column gives

$$0=-\int_0^H w\frac{\partial M}{\partial z}\,dz-MV\Big|_0^H+\int_0^H wG\,dz+\int_0^H Mw\frac{\partial \ln \rho}{\partial z}\,dz. \tag{5}$$

The second term on the right of (5) is the precipitation rate at the base of the updraft because at the top $M\leq 0$ and, therefore, $V=0$ there; the third term is the condensation rate in the vertical column of unit cross section.

The first term on the right is better understood after integration by parts, i.e.,

$$\int_0^H w\frac{\partial M}{\partial z}\,dz=\int_0^H \frac{\partial}{\partial z}(wM)dz-\int_0^H M\frac{\partial w}{\partial z}\,dz \tag{6}$$

$$\int_0^H w\frac{\partial M}{\partial z}\,dz=wM\Big|_0^H-\int_0^H M\frac{\partial w}{\partial z}\,dz. \tag{7}$$

The first term on the right of (7) vanishes because $w=0$ at both $z=0$ and $z=H$. And the equation of continuity for air implicit in equation (1) states that $\partial w/\partial z$ in the second term on the right of (7) is given by

$$\frac{\partial w}{\partial z}=-\left(\frac{\partial u}{\partial x}+\frac{\partial v}{\partial y}+w\frac{\partial \ln \rho}{\partial z}\right). \tag{8}$$

Substitution of (8) and (7) into (5) yields

$$-(MV)_{z=0}=R_{z=0}=\int_0^H wG\,dz-\int_0^H M\left(\frac{\partial u}{\partial x}+\frac{\partial v}{\partial y}\right)dz. \tag{9}$$

Equation (9) is a reminder that the horizontal divergence of the wind is implicit even in the one-dimensional forms of equation (1). The last term in equation (9) may be positive, negative, or zero, and is largely dependent on the ratio of characteristic fall speed to the characteristic updraft.[3] The relative contribution of the last term in (9) is usually most important in the strong updraft situations where $M$ is increased in greater proportion than $w$ (because the fall speed of precipitation usually increases only a little with a large increase of intensity). From another point of view, note that it is when $V$ is relatively small and only slowly varying, as in snow, that $M$ is relatively quite large near the ground where the divergence is negative, and that the last term in (9) contributes substantially to the precipitation rate near the center of areas of widespread precipitation. In such cases the precipitation rate significantly exceeds that defined by the condensation term alone. Any excess of precipitation over condensation near an updraft core is, of course, accompanied by a deficit in areas away from the core.

In other cases, particularly where the melting zone, associated with a five-fold increase of particle fall speeds, coincides with the level of no horizontal divergence of the wind, the steady precipitation rate at updraft centers may be somewhat less than the condensation rate there. A physical approach to the results summarized by equation (9) is illustrated in figure 5 of [4].

These results should be of some value for relating updraft velocities to observed precipitation rates and radar echo intensities.

## 4. ASSUMPTIONS IMPLICIT IN THE RELATIONSHIP $N(V+w)$=CONSTANT

The equation

$$N(V+w)=\text{constant} \tag{10}$$

where $N$ is the concentration of precipitation particles at various points along a vertical, has been used by several

[3] Equation (9) is the same whether the atmosphere is assumed to be compressible or incompressible. However, the distribution of the quantities therein and the magnitude of the integrals vary somewhat with considerations of compressibility. See, for example, figure 1 of [4].

investigators, including the author [3], as a conservation law suited for a study of precipitation models. Some published work concerning precipitation mechanisms rests on one or more implications of this equation (10), even where (10) is not explicitly invoked. Although many important limitations of (10) and its corollaries have long been recognized, it has not been generally realized that this equation often stands in violation of fundamental principles of continuity.

The conditions under which (10) is valid can be examined by reference first to

$$\frac{\partial M}{\partial t}=\frac{dM}{dt}-(V+w)\frac{\partial M}{\partial z}, \tag{11}$$

derived immediately from first principles. Equation (11) states merely that in the absence of horizontal advection, the local change of $M$ is the sum of individual and vertical advective changes. Substitution for $\partial M/\partial t$ from the one-dimensional form of (1) gives

$$\frac{dM}{dt}=wG-M\frac{\partial V}{\partial z}+Mw\frac{\partial \ln \rho}{\partial z}. \tag{12}$$

In (12), let $M=Nm$, where $m$ is the mass of each particle in a collection of $N$ particles. Then

$$m\frac{dN}{dt}+N\frac{dm}{dt}=wG-mN\frac{\partial V}{\partial z}+mNw\frac{\partial \ln \rho}{\partial z}. \tag{13}$$

Suppose that combination and breakup processes among precipitation particles are weak and that the condensation-evaporation term contributes to the mass of individual particles, but not to their number; i.e., precipitation particles grow or diminish in size, but are neither created nor destroyed. This assumption may be applicable, for example, to the further development of a packet of small hail. Then equation (13) can be separated into two equations:

$$m\frac{dN}{dt}=-mN\frac{\partial V}{\partial z}+mNw\frac{\partial \ln \rho}{\partial z} \tag{14}$$

and

$$N\frac{dm}{dt}=wG. \tag{15}$$

The temporal changes of particle concentration along the path of an individual packet are given by

$$\frac{dN}{dt}=\frac{dz}{dt}\times\frac{dN}{dz}=(V+w)\frac{dN}{dz}. \tag{16}$$

Divide (14) by $m$, substitute (16) into (14), multiply by $\partial z$, and rearrange terms to obtain

$$\frac{\partial N}{N}=-\frac{\partial V}{V+w}+\left(\frac{w}{V+w}\right)\frac{\partial \rho}{\rho}, \tag{17}$$

which applies along a vertical at any time if the distribution state is steady, but should be restricted to the flow following an individual packet (individual derivatives) when the distributions are unsteady. In the idealized case of descent at constant fall velocity through a constant updraft, the term $\partial V/(V+w)$ in (17) is zero, but there is still a decrease in the number of particles per unit volume because in a compressible atmosphere, effects of horizontal divergence, measured by the third terms in equations (14) and (17), accompany updrafts that are invariant with height. The effect of the third term in (17) must in nature be more or less compensated by the tendency of precipitation fall speeds to decrease as the particles descend into air of increasing density.

*Only if $w$ is constant or, at least, everywhere quite small in comparison to $V$,* can the integral of equation (17) without the compressibility term be represented by equation (10). The assumption that $w$ is constant or everywhere small compared with $V$ is quite similar to the assumption that the horizontal or vertical divergence of the wind is small compared with the vertical divergence of $V$. This may be clearly understood after consideration of the vertical derivative of equation (10);

$$N\left(\frac{\partial V}{\partial z}+\frac{\partial w}{\partial z}\right)+(V+w)\frac{\partial N}{\partial z}=0. \tag{18}$$

Equation (18) contains the term $N(\partial w/\partial z)$, which is properly omitted, since it is practically canceled by effects of horizontal divergence, as shown by the equation of continuity for air. Note that the term $N(\partial w/\partial z)$ has no analog in equation (4). Use of equation (10) across a layer where $w$ varies implies neglect of horizontal divergence and violation of continuity principles; such use will be associated with important errors unless the magnitude of air speed changes is small.

The inherent similarity of assumptions (1) that steady precipitation and condensation rates are equal and (2) that equations like equation (10) can be applied to the study of precipitation, can be understood in terms of this discussion. As fall speed increases relative to $w$ and $M$, the integral of the horizontal divergence times $M$ in equation (9) and the errors associated with equation (10) become relatively small, and these assumptions are satisfactory.

Equation (10) is valid for estimating the change of $N$ accompanying important changes of $V$ which occur over such a short interval that variations of $w$ are negligible, or over larger intervals in which $w$ is everywhere much smaller than $V$. The application of equation (10) is possibly justified in the zone in which snow melts to form rain with an approximately fivefold increase of particle fall speed, especially when the effects of breakup of melting particles can otherwise be included or shown to be small. (See sec. 7B and table 1 of [4].) Other possible applications are to layers in which updraft speeds are uniform and where $N$ and $V$ can be estimated at at least

one height in the layer. In no event, of course, are equations (10) and (18) even crudely sufficient for application over a region where $w$ varies and $(V+w)$ passes through or near zero. They are not applicable, for example, to the study of hail. Where $w$ attains about the same magnitude as $V$, a more accurate integration of equation (18), rather than equation (10), must be employed.

It is, at least, of academic interest to note that equations (14) and (15) with boundary and initial conditions uniquely define $m$ and $N$ at all heights when the masses of the particles are expressed in terms of their fall velocities. The relation $V=-130D^{1/2}$, where $V$ is in m./sec. and $D$ is in meters (Spilhaus [15]), can be used to give $V=-130(6m/\pi)^{1/6}$ (m./sec.), where $m$ is in grams. Use of this relationship with appropriate boundary and initial conditions allows solution of (14) and (15) for $m$ and $N$ where the updrafts are known at every height and time—or, knowledge of $m$ and $N$ along the trajectory of $M$ permits the determination of updraft distributions. Horizontal advection when present simply requires that equations (14), (15), and (17) be applied along the nonvertical trajectory of precipitation descending through the atmosphere. These equations can be viewed as a theory of monodisperse-size-distributed precipitation, applicable in a layer where breakup and combination processes are weak and where fall velocities are everywhere larger, but not necessarily much larger, than the updrafts.

## 5. TWO-DIMENSIONAL SOLUTIONS

### A. INSTANTANEOUS-EVAPORATION OF CONDENSATE IN SUBSATURATED AIR

This section discusses time-dependent distributions of water substance and the methods for deriving them in two model cases where condensate fall speeds are twice the magnitude of maximum updrafts and in two cases where fall speeds are half the maximum updrafts. Two sets of solutions are presented for each updraft-fall speed ratio: one set where there is instantaneous evaporation of condensate in subsaturated air; the other where there is no evaporation of condensate in subsaturated air. The most nearly natural cases must lie between these extremes. The methods for obtaining solutions are instructive of basic interactions between air motions and water transport.

The following equations have been considered in connection with the two-dimensional solutions:

$$\frac{\partial M}{\partial t}=-u\frac{\partial M}{\partial x}-(w+V)\frac{\partial M}{\partial z}-M\frac{\partial V}{\partial z}+wG, \tag{19}$$

$$w=\frac{4w_{max}}{H}\left[z-\frac{z^2}{H}\right]\cos\frac{2\pi x}{L}, \tag{20}$$

$$u=\frac{2Lw_{max}}{H}[2z-1]\sin\frac{2\pi x}{L}+f(z), \tag{21}$$

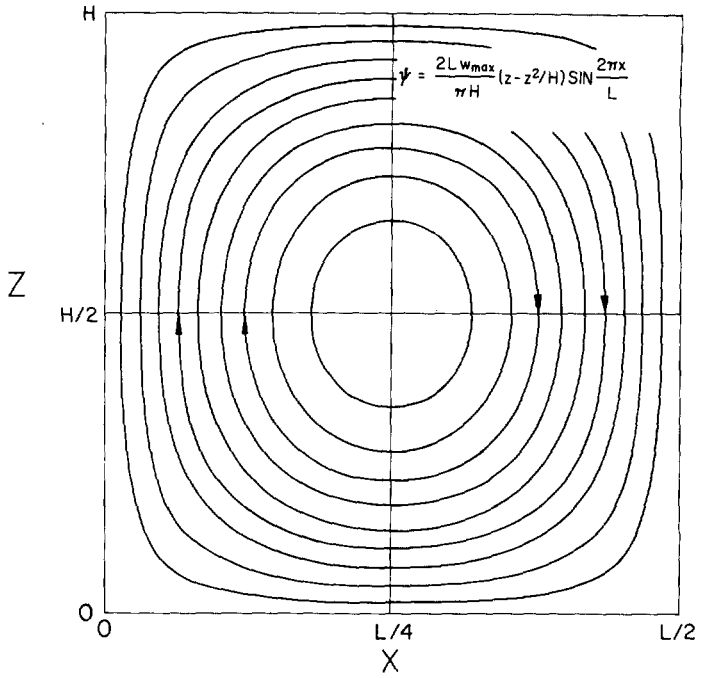


FIGURE 3.—Streamlines of the wind field corresponding to equations (20), (21), and (22) with $f(z)=0$, over the range $0\leq x\leq L/2$.

$$\psi=\frac{2Lw_{max}}{\pi H}\left[z-\frac{z^2}{H}\right]\sin\frac{2\pi x}{L}-\int_0^H f(z)dz. \tag{22}$$

Equation (19) applies to an incompressible atmosphere and equations (20) and (21) satisfy the corresponding continuity condition, viz, $\partial u/\partial x+\partial w/\partial z=0$. In equations (21) and (22), $f(z)$ is the nondivergent environmental wind. These equations are solved in the layer $0\leq z\leq H$, with $M$ specified at $z=H$. The limits of integration in the horizontal direction are usually chosen so that there is no horizontal wind at these boundaries, for example, $nL/2\leq x\leq(n+1)L/2$, where $n$ is an integer or zero when $f(z)=0$. Then the one-dimensional solutions already discussed exist along the verticals at the horizontal limits of the problem area, and no boundary conditions other than the value of $M$ at $z=H$ need be specified at these limits. Other alternatives are both practical and interesting but are not discussed further here.

The wind field described by equations (20), (21), and (22) with $f(z)=0$ is shown by figure 3. With $V$ constant for $M>0$ and $V=0$ wherever $M<0$, and with initial condition $M=0$, boundary condition $M(H)=0$, and $G=$constant, equation (19) has been solved by finite difference methods for the field of $M$ at various times. As noted in the introduction, these assumptions concerning $M$ and $V$ imply the instantaneous evaporation of condensate in any subsaturated air into which it falls. The top rows of figures 4 and 5 show solutions for two relationships between the uniform fall speeds of condensate and the maximum updrafts. Details concerning the method of solu-

tion and discussion of these solutions and associated budget parameters are contained in section 5 of [5].

B. NO-EVAPORATION OF CONDENSATE IN SUBSATURATED AIR

Equation (19) can be solved in a modified way that admits of no evaporation of condensate once formed. Such a method is interesting because in subsaturated air the most nearly natural case must lie between the extremes of no evaporation and instantaneous evaporation of precipitation. The revised method for solving (19) is based on the following.

Consider two sets of equations, one set for condensate and one for vapor. Each set constitutes a restatement of the same conservation principle expressed by (19). We have

$$\frac{dM}{dt}=wG,\ \begin{matrix}M\geq 0\\ q=0\\ w>0\end{matrix} \quad (23a); \qquad \frac{dz_M}{dt}=w+V,\ M>0 \quad (23b)$$

$$\frac{dq}{dt}=wG,\ q<0 \quad (24a); \qquad \frac{dz_q}{dt}=w,\ q<0 \quad (24b)$$

where $M$ is now the air's precipitation content, always positive or zero, and $q$ is the vapor density minus the saturation vapor density, zero in saturated air and a negative quantity in unsaturated air. Note that equation (23a) is applied only in saturated updrafts (elsewhere $dM/dt=0$); (23b) is applied to determine the motion of $M$. Since $q=0$ in all saturated updrafts, equations (24a) and (24b) are of concern only in following the motion and changes of $q$ in unsaturated air. The term $M\partial V/\partial z$ does not appear in equation (23a) because $V$ is assumed constant for condensate. In areas where $M>0$ and $q<0$, it is necessary to apply both sets of equations. There is no evaporation when the values of $M$ and $q$ are not added at points where $q$ is negative and $M$ positive.

The two-dimensional solutions have been determined by combining the host of one-dimensional solutions applicable along the trajectories (also streamlines in these cases of steady wind fields) of $M$ and $q$. Figure 6 illustrates the streamlines for $V/w_{max}=-2$. Note that the streamlines of $q$ are identical with those of the wind field, and that equations (24a) and (24b) can be combined and integrated to yield $q=q_0+G\Delta z$. The solutions for $q$ are thus given by the vertical displacements along air-streamlines; these displacements have been determined by finite-difference and graphical methods. The time-height relationships for $M$ and the steady-state profile of $M$ along each $M$-streamline have also been determined by combinations of numerical and graphical techniques. The results for $M$ are summarized in figure 7, which is the principal basis for the graphical development of time dependent solutions in this case.

To obtain the no-evaporation solutions, it is necessary to know the boundary separating air where $q=0$ from that where $q<0$; this is defined by the locus of particles that have risen in the updraft part of the cell as much as they had previously descended in the downdraft portion. Figure 6 shows, for three times, this demarcation as determined by finite-difference methods in the interior of the circulation cell and by exact methods on the lower cell boundary. Along the streamlines for condensate, growth of $M$ is assumed to follow the curves of figure 7 only so long as $M$ is in air that is saturated. As soon as $M$-parcels cross the boundary separating saturated from unsaturated air, i.e., separating air where $q=0$ from air where $q<0$, growth of $M$ ceases and the remainder of the $M$ history is due to advection only. The no-evaporation solutions where $V/w_{max}=-2$ are shown in the lower row of figure 4.

The solutions of the problem where $V/w_{max}=-1/2$ are shown in the lower row of figure 5; these have been obtained in the same manner as described above, but with somewhat greater difficulty, especially where the streamlines of $M$ are loops. (See, for example, [5] figure 7.)

The solutions in upper and lower rows of figures 4 and 5 must differ only where precipitation falls into air which has been rendered unsaturated by the air's prior descent. Other differences between corresponding diagrams, where not attributable to drafting uncertainties, are due to use of a smoothing equation in the program for digital computation of instantaneous evaporation cases. Since large numerical differences between solutions of instantaneous-evaporation and no-evaporation models are confined to small areas in the cases shown, it has not seemed worthwhile to extend to the present study the detailed budget computations discussed in [5].

The solutions shown can be scaled to any distribution of atmospheric parameters which differ by constant factors from those used here, as discussed in [5]. For new scale height $\mathscr{H}$, new generating function $\mathscr{G}$, new vertical air speed $\mathscr{W}_{max}$, and new fall velocity $\mathscr{V}=\mathscr{W}_{max}V/w_{max}$, the new solutions denoted by $\mathscr{M}$ are given by $\mathscr{M}=M\mathscr{G}\mathscr{H}/GH$ which occur at new times $\mathscr{T}=T\mathscr{W}_{max}\mathscr{H}/w_{max}H$. (See sec. 2 of [5].) The solutions for given $G$, $H$, and $w_{max}$ can be applied to any horizontal scale, since the equation of continuity for air requires that stretching of the horizontal scale be associated with an equivalent stretching of the horizontal wind speed, when the vertical air speed is unchanged.

The particular wind and water fields used here have some features demonstrably inconsistent with thermodynamic principles. For example, thermal changes must closely follow moist and dry adiabatic processes in saturated updrafts and unsaturated downdrafts, respectively. Since updrafts and downdrafts have equal intensity in our model wind field, the descending current for a representative conditionally unstable initial lapse rate becomes considerably warmer than the ascending current at corresponding levels, long before the circulation has progressed to the illustrated final stages. Therefore, another model should be considered, say a radially symmetric

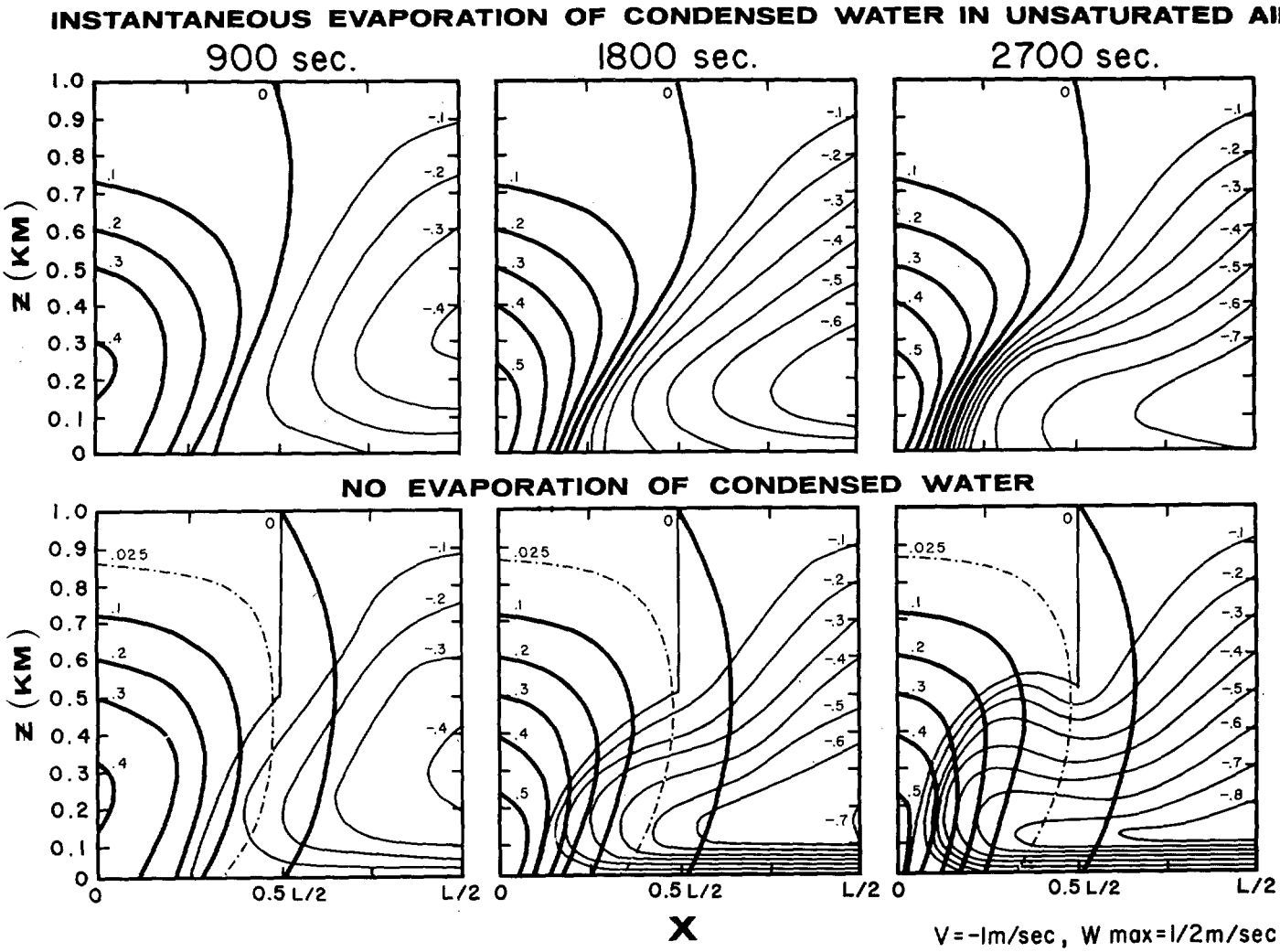


FIGURE 4.—Analyzed fields of water content based on a steady wind field of shape as shown in figure 3, maximum vertical air speed of 0.5 m./sec., uniform condensate fall speed of 1 m./sec., and lapse of saturation vapor density of 1 gm. m.$^{-3}$ km.$^{-1}$ At time =0, the atmosphere is everywhere saturated. The heavy lines show the concentration of condensate in gm./m.$^3$ and the light lines show the amounts of vapor required to saturate the air. The upper row illustrates the case in which condensate evaporates instantly when it falls into air that has become unsaturated by virtue of its history in the descending branch of the circulation; the lower row illustrates the case in which there is no evaporation of condensate. The time 2700 sec. marks substantial overturning of the air in the circulation cell. Further discussion is in the text.

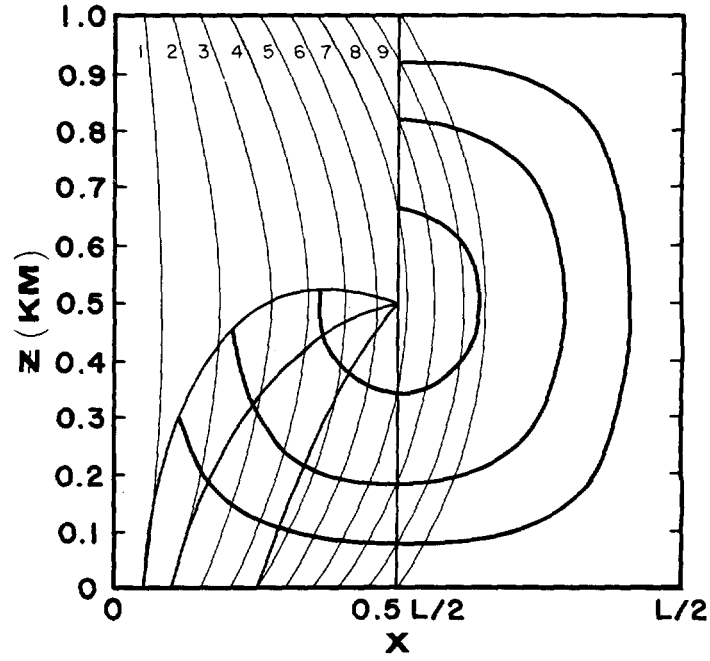


FIGURE 6.—Streamlines of condensate (light) and of vapor (heavy lines corresponding to those shown in figure 3). The paths of condensate apply to the case $V/w_{max}=-2$. The boundary separating saturated from unsaturated air is shown for times $t=0$, 0.45 $H/w_{max}$, 0.90 $H/w_{max}$, and 1.35 $H/w_{max}$ by the lines of intermediate weight. Integers on the streamlines of condensate refer to the steady-state solutions shown in figure 7.

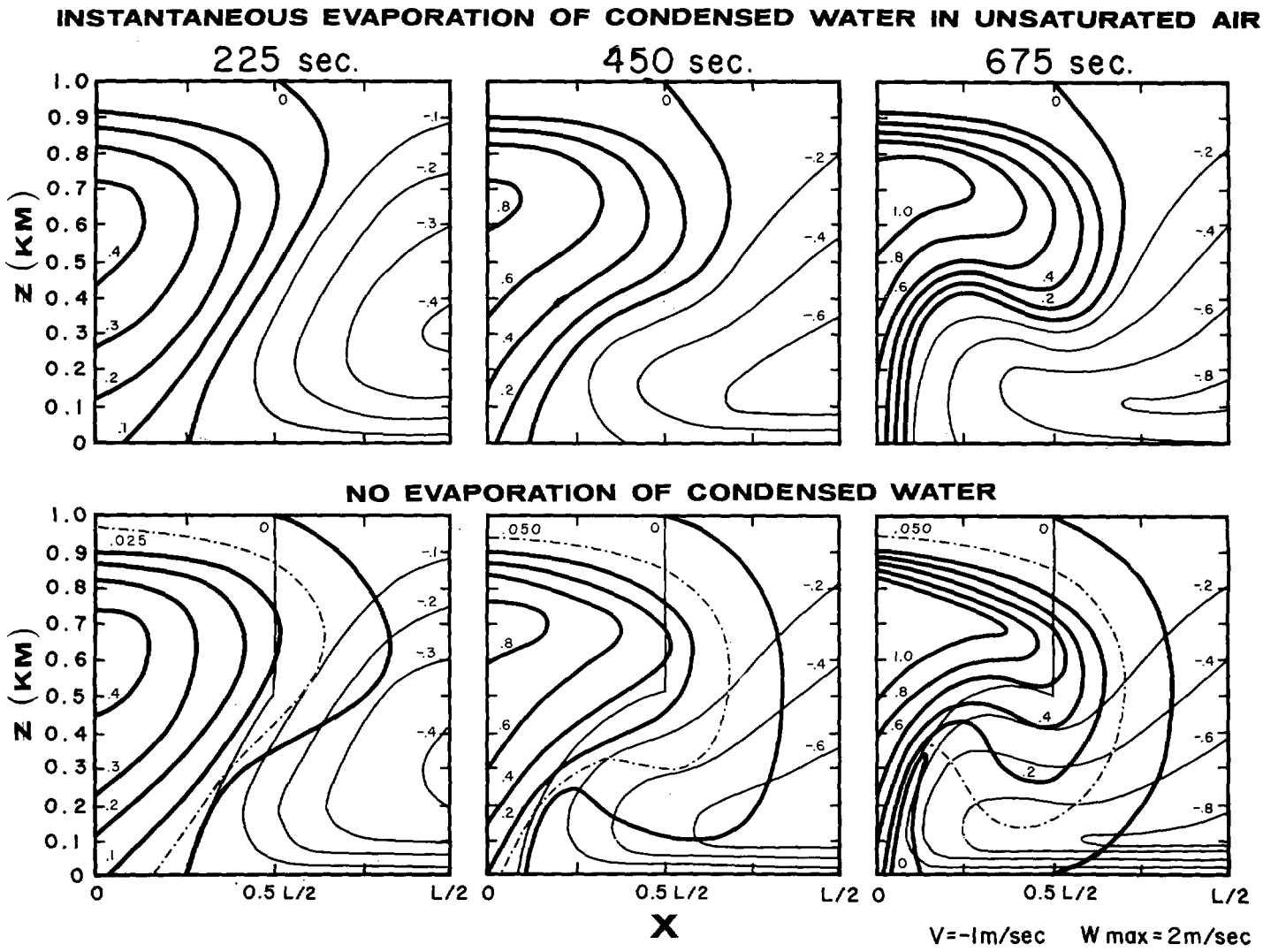


FIGURE 5.—Same as figure 4, except that $w_{max}$=2 m./sec. and the time for substantial overturning of the air is reduced to 675 sec.

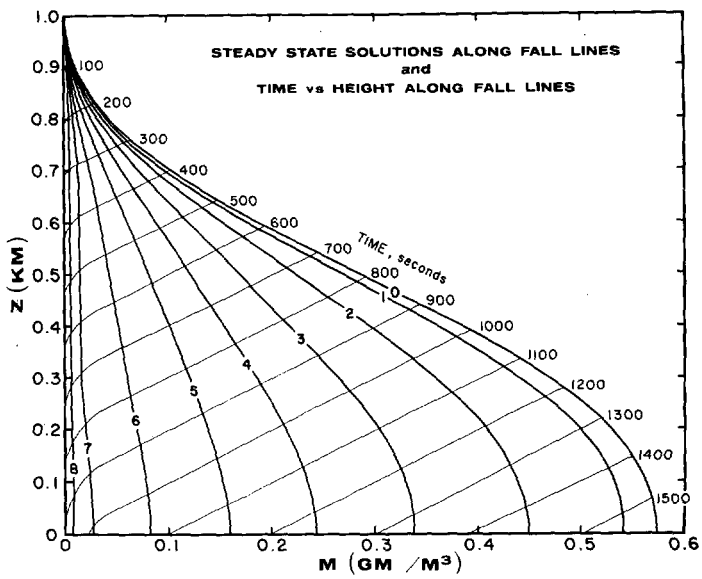


FIGURE 7.—Diagram used to determine time-dependent distributions of condensate illustrated in lower row of figure 4. The numbered lines descending from the upper left corner are the steady-state $M$-distributions along the streamlines denoted by corresponding integers in figure 6. The time intervals occupied by $M$-packets descending from one height to another are given by the lines ascending from the left.

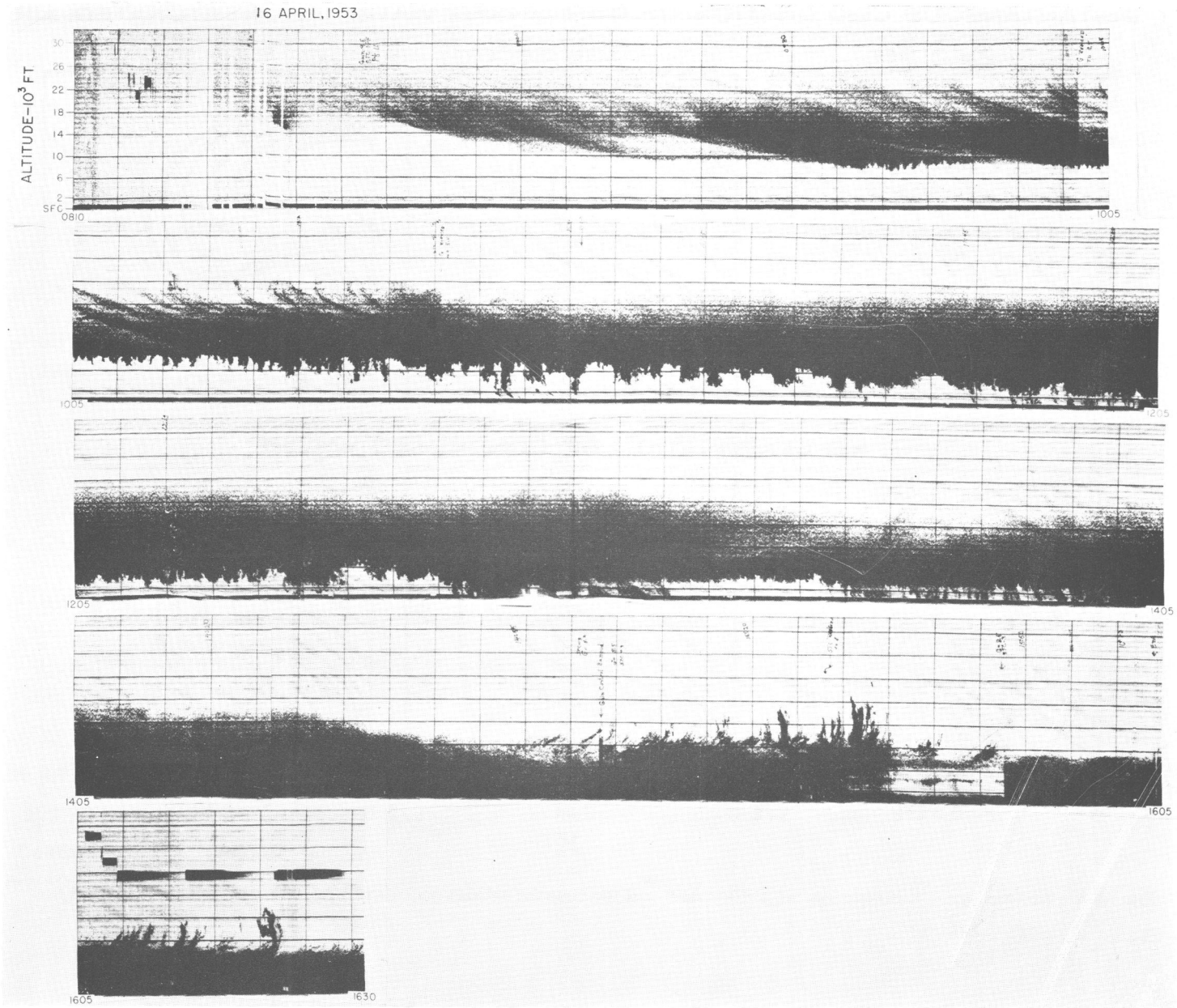


FIGURE 8.—Photograph of the time-height record made with a 1.25-cm. vertically pointing radar. Vertical lines indicate 5-min. time intervals. Precipitation stalactites are most pronounced in the second row. Weak generators and trails also occur in the second row; trails without detectable generators occur in the first row; and strong generators are in the fourth row.

type, wherein the downdraft area is much more widespread and the downdraft intensities correspondingly more gentle than the updrafts. The solutions in such cases can be produced in just the manner already shown. At the updraft center, the solutions are the same as those already discussed when the vertical velocity distribution is the same as that given by equation (20); elsewhere, the principal differences are described in terms of a reduction of the linear extent of the inflow from the descending branch of the circulation, decreased linear extent of the outflow aloft, and somewhat higher precipitation efficiencies in the evaporation cases, since less dry air is interposed between precipitation aloft and the ground.

It is obvious that a higher percentage of the condensate formed in updrafts must reach the ground when updrafts and compensating downdrafts are separated by great distances, and when downdrafts are spread over wider area and are therefore comparatively weak. It is also obvious that for a given circulation in an initially unsaturated atmosphere, more of the water condensed in updrafts will evaporate again before reaching the ground than in the cases illustrated here. Of course, many kinds of circulation can be imagined, and a study incorporating thermodynamic principles quantitatively would be necessary to determine which ones probably occur.

The method of solution by use of streamlines rather

than a rectangular grid is the more inherently accurate and can be modified at the cost of added complexity to take account of various rates of evaporation. For example, the streamline method can be used to study instantaneous evaporation by adding values of $M>0$ and $q<0$ algebraically after a short time interval to define a new field of $M+q$ from which the new locus of $M+q=0$ can be determined. It seems however, that little would be gained by introduction of complexities of this kind without generalization of the assumptions discussed in the introduction to this study.

## 6. THE KINEMATIC BASES OF GENERATORS

*Generator* is the name given to the sources of precipitation streaks (usually snow) observed visually and by radar; like practically all precipitation sources, generators are identified with vertical circulation of air. A history of a generator circulation and the processes affecting it and its associated trail of snow is incorporated in the water content distribution. Generators and trails have been studied extensively by Marshall [10], Atlas [1], and Douglas, Gunn, and Marshall [2]. Weak generators are shown in figure 8. In this section, the application of kinematic theory is shown to provide bases for estimating the lifetime of generators and the strength of their vertical currents from radar and visual observations.

In this investigation, it has been assumed that the generating circulation is given by equations (20), (21), and (22) with $f(z)=0$; the environmental wind does not vary with height in the generating layer. In figure 9, the wind shear below the generating level has been taken as 5 m. sec.$^{-1}$ km.$^{-1}$ The generating cells are 1 km. deep and $G$, in equation (19), has been taken as 0.7 gm. m.$^{-3}$ km.$^{-1}$, a representative value for winter near the 600-mb. level. Precipitation in the trails falls 1 m./sec., representative of snow, without growth or diffusion. The water density distributions within the cells have been scaled from those illustrated in the upper rows of figures 4 and 5 according to the discussion given in section 5, and the trails plotted in accordance with the equations that relate fall velocity and wind shear to position relative to the generators, as discussed in the references.

With the given assumptions, all the possible shapes of the $M$-distributions are implied by the possible range of the ratio $V/w_{max}$. The ratio $-V/w_{max}=2$, is given by the patterns at the left of figure 9, and $-V/w_{max}=1/2$ is given by the patterns at the right. The labeled water contents are for maximum updrafts of 0.5 and 2 m./sec., respectively. In both cases, the circulation starts at time $t=0$ and proceeds until $t=1.44\ H/w_{max}$ when substantial overturning has occurred,[4] and then ceases. In these models, the precipitation that descends into air that becomes subsaturated in the generator downdrafts evaporates instantly.

Many features of the model distributions in figure 9 are similar to the trails observed visually or by radar. In both model distributions, the maximum value of $M$ is inside the generator during the early, active stages and in or near the generator during most of the period of simple fallout. Second, water content distributions in the trail of the generator with weak updrafts are constant or slowly varying over the trail length, in good qualitative agreement with observations of many trails. The short trails and large condensed water contents of the model generator on the right are suggestive of many observations that have been subjectively and qualitatively associated with relatively vigorous convection. Third, the lifetimes of the model generators confirm our mostly casual observations that generators seen on radar and cirrus and altocummulus floccules seen visually, are often tracked for tens of miles and as many minutes.

Study not detailed here shows that the most prominent features of the water distribution shapes in the left and right of figure 9 are little different in association with respectively weaker and stronger updrafts. However, where $-V$ and $w_{max}$ are about equal, the shapes of the condensed water distribution are very sensitive to the value of $V/w_{max}$. This indicates that generator and trail observations might be usefully separated into classes where updrafts are either less than or greater than the terminal falling speeds of the precipitation involved. A uniform long trail such as that illustrated on the left of figure 9 is reasonable only when the fall speed of the precipitation exceeds the updraft; the frequent occurrence of this type of observation indicates the prevalence of convective circulations in snow with vertical speeds rather less than 1 m./sec. The same core-water content distributions and conclusions are valid if the wind field is radially symmetric or if the generator downdrafts are more widely dispersed in a two-dimensional configuration than assumed here.

The solutions suggest inquiry into other quantitative relationships between the possible observable cell and trail parameters and the ratio $V/w_{max}$. Where the core updraft profile is parabolic with height and precipitation fall velocities are uniform as above, and where the air circulation is steady from $t=0$ to $t=CH/w_{max}$, the following relationship gives the duration of steady precipitation at the midpoint of the generator base:

$$t_s=\frac{H}{w_{max}}\left[C-(-K-1)^{-1/2}\tan^{-1}(-K-1)^{-1/2}\right], \quad (25)$$

where $K$ is equal to $V/w_{max}$ and is less than $-1$. When there is simple descent in the region below the generator, $t_s$ may be related to the vertical depth $D_s$ of the part of a trail with a steady core intensity by the relation $D_s=t_sV$, and the duration $t$ (of the whole precipitation-releasing circulation) might be empirically related to the total trail depth by the relation $D=tV$.

The numerical value of the steady core-water content at the generator base and in the trail under the same conditions as above is given by

$$M=\overline{G}HK\,(-K-1)^{-1/2}\left[1-\tan^{-1}(-K-1)^{-1/2}\right], \quad (26)$$

where $\overline{G}$ is the average value of $G$ in the generator layer.

[4] $1.44\ H/w_{max}=48$ and 12 min., for left and right patterns, respectively.

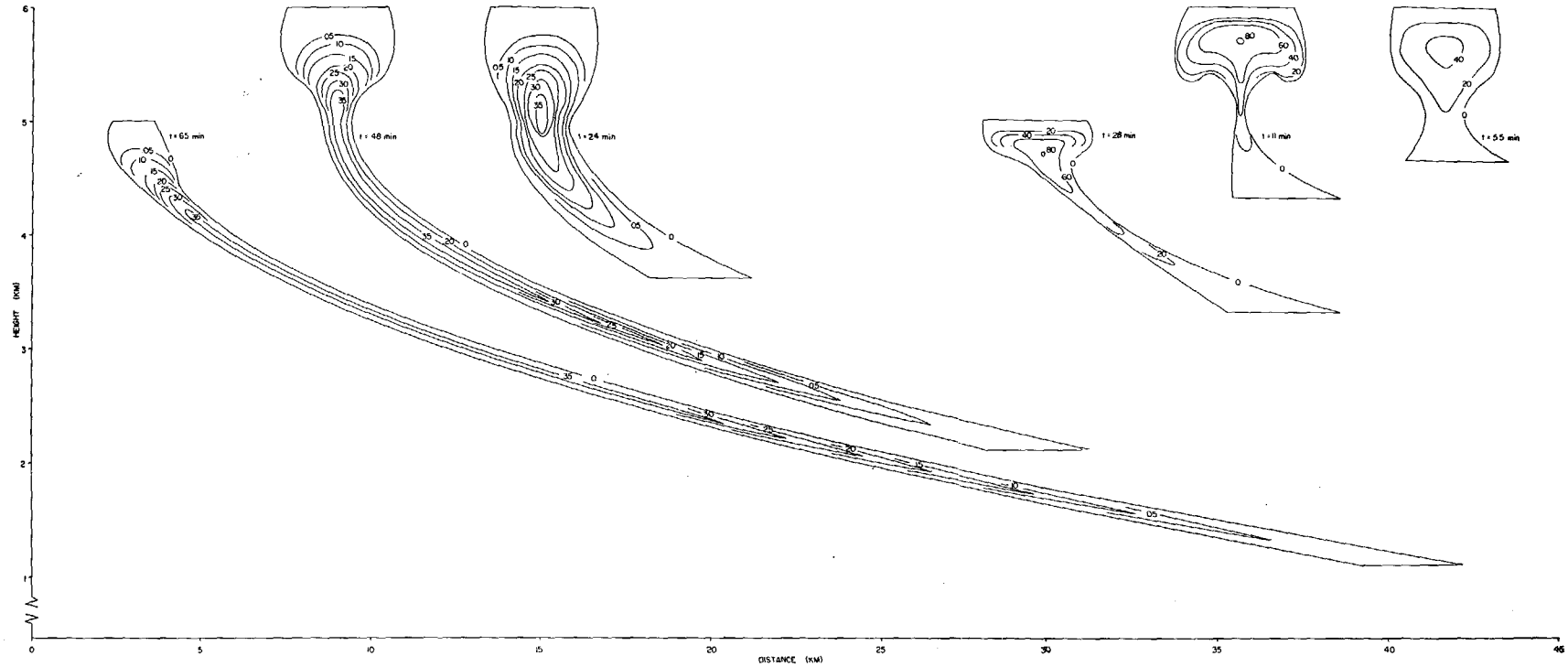


FIGURE 9.—Model generators and their trails. The fall speed of precipitation is 1 m./sec. and the air circulations are as pictured in figure 3, extended over the interval $-L/2 \leq x \leq L/2$. Maximum updrafts of 0.5 m./sec. apply to the figures on the left, and 2 m./sec. apply to those on the right. The wind shear beneath the generators is 5 m. sec.$^{-1}$ km.$^{-1}$ The condensation function is constant at 0.7 gm. m$^{-3}$ km.$^{-1}$ and isopleths of water content are labeled in gm./m.$^3$ In each triad, the separate pictures can be viewed as different stages in the life of one generator or as three generators in different stages. The middle picture in each set shows the distribution of condensed water at the time the circulating air has overturned and the convective air motion has stopped.

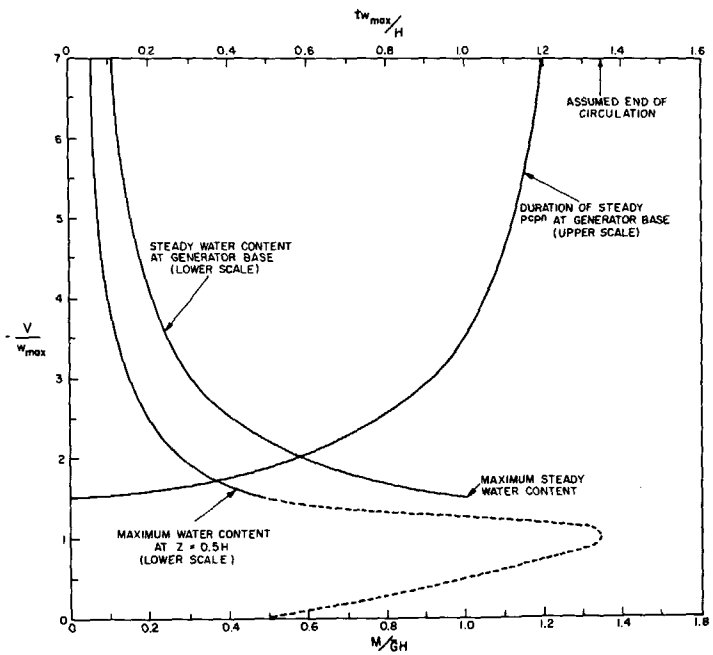


FIGURE 10.—Parameters of generators and their trails. The duration of steady precipitation and the maximum steady water content at the generator base assume cessation of the circulation at $t=1.35\ H/w_{max}$.

The maximum steady water content at the generator base for a fixed amount of air overturning occurs when $K$ is such that steady conditions within the generator core are just attained when the air circulation stops. When $K \geq -1$, there is no steady state; the methods used in these cases to compute the time-dependent $M$-distributions in the updraft cores are discussed in section 1. These methods have been used to obtain, in figure 10, the dashed part of the curve which shows the maximum water contents at a point midway between base and top of the generator.

## 7. THE STALACTITE PROBLEM

Stalactites, as observed by vertical-pointing radar, are illustrated in figure 8. The best published discussion of stalactites is probably contained in Douglas, Gunn, and Marshall [2]. These radar-observed phenomena occur when stratiform precipitation descends into a dry air layer, thereby destabilizing it by evaporative cooling. The depth to which overturning of the air then occurs and the extent of the associated downward projections of precipitation (stalactites) appear to be governed by such factors as the initial vertical distributions of temperature and moisture and the precipitation rates. In the stalactite layer, precipitation descends most rapidly in the downdrafts and is slowed or suspended in the updrafts. Moisture descends irregularly, and new convective cells probably arise beneath the old as the precipitation lowers. Stalactites are more pronounced in snow than in rain, in part because evaporation from relatively fast-falling rain is associated with a smaller vertical gradient of the cooling rate than snow is. In this section the application of kinematic theory shows that the stalactite observations may be explained by vertical currents of about 1 m./sec.

Equations (19), (20), (21), and (22) describe a model stalactite situation provided that the condition $M=$ constant is applied at $z=H$ and the interior of the circulation cell initially contains dry air. The outstanding feature of this problem is the $M$-discontinuity that separates descending condensate and the dry air beneath. A proper solution of the instantaneous evaporation case includes accurate delineation of this boundary. However, the digital techniques described in [5] are inadequate in the presence of this discontinuity, and the extension of the computational method used to obtain the solutions shown in the lower rows of figures 4 and 5 is too laborious for hand calculation and has not been programed for a computer.

A simpler problem is defined by the assumption that evaporation is very slight (just enough to start the convective cell and to keep it going!) and that the leading edge of precipitation is therefore given by the locus which connects points descending at speed $(V+w)$ along streamlines of $M>0$. For the two-dimensional example with $-V=2w_{max}$, isochrones of the leading edge starting with $t=0$ at $z=H$ are illustrated in figure 11. An analytical expression for the stalactite length in this no-evaporation case is given by $V(t_u-t_d)$, where $t_u$ and $t_d$ are the times required for condensate to traverse the updraft at $x=0$ and the downdraft at $x=L/2$, respectively. Where $V$ is constant and the vertical $w$ distribution is parabolic, the stalactite length $S$ is given by

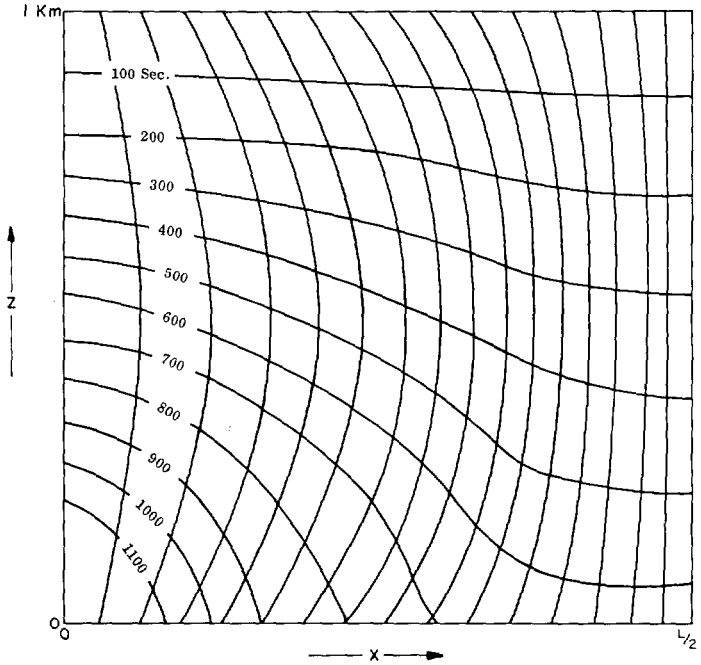


FIGURE 11.—Horizontally tending lines are isochrones marking the leading edge of nonevaporating precipitation which descends from $z=H$ at $t=0$. Descent through the wind field where $V/w_{max}=-2$ is along the vertically tending streamlines. Time labels apply if $V=-1$ m./sec., $w_{max}=0.5$ m./sec., and $H=1$ km.

$$S=KH\left[\frac{1}{\mathscr{K}^-}\tan^{-1}\frac{1}{\mathscr{K}^-}-\frac{1}{4\mathscr{K}^+}\ln\frac{2(1+\mathscr{K}^+)-K}{2(1-\mathscr{K}^+)-K}\right], \quad (27)$$

where $K=\dfrac{V}{w_{max}}<-1$, $\mathscr{K}^-=(-1-K)^{1/2}$, and $\mathscr{K}^+=(1-K)^{1/2}$.

The graph of equation (27) is given in figure 12.

A more probable wind structure associated with stalactites consists of a central core of strong downdrafts surrounded by a ring of much weaker updrafts. At some distance from the strong downdraft, the vertical motion is zero. In this case, the stalactite length is deduced from study of precipitation descent in the downdraft core and in the no-draft region considerably removed from the core. The applicable equation, whose plot is also illustrated in figure 12, is the same as equation (27), except that the term $(1/\mathscr{K}^-)\tan^{-1}(1/\mathscr{K}^-)$ is replaced by $1/K$.

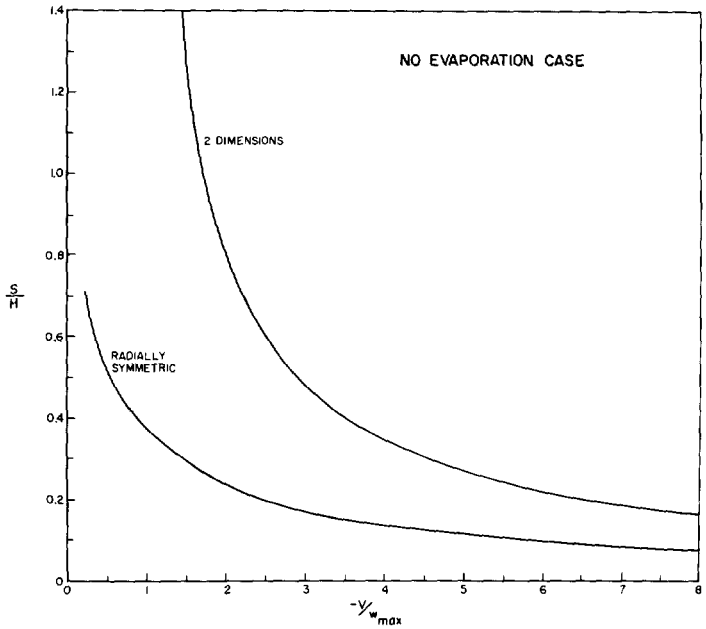


FIGURE 12.—The ratio of stalactite length $S$ to cell depth $H$ is plotted against $-V/w_{max}$ for cases of no evaporation in two kinds of wind fields discussed in the text.

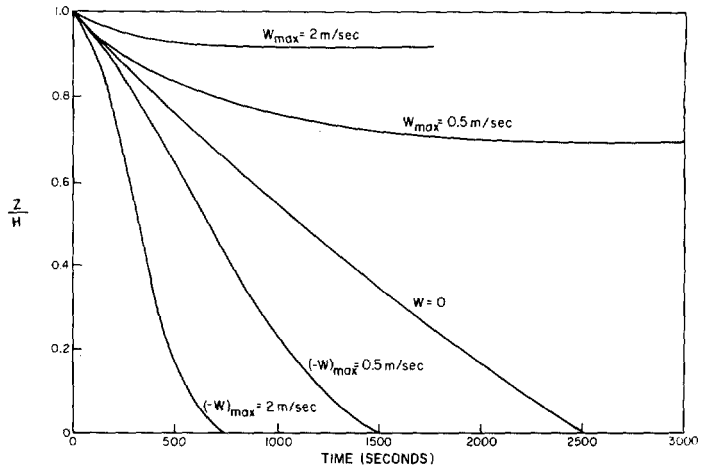


FIGURE 13.—The time for precipitation falling at 1 m./sec. to descend through a depth $H=1$ km. is indicated for two downdrafts (lower curves), two updrafts, and a quiet atmosphere. In each case, precipitation is assumed to evaporate instantly in subsaturated air, the initial distribution of $M$ is $M=-2+(z/H)$ (gm./m.$^3$), and the upper boundary value is $M=1$ gm./m.$^3$

The no-evaporation plots in figure 12 represent conservative estimates of stalactite length, in that greater lengths are suggested by an elementary study of evaporative effects, described below. With this conservatism of the present theory in mind, consider $V=-1$ m./sec. in the radially symmetric case, and note that a circulation cell with maximum downdrafts of 2 m./sec. would give stalactites half the depth of the cell. If updrafts are locally as widespread and as strong as the downdrafts, the maximum stalactite lengths could be as great as the cell depths with maximum vertical currents of only 0.5 m./sec. If the atmospheric circulations in depth are about the same as their horizontal spacing, then the stalactite observations themselves suggest that vertical drafts of about 1 m./sec. are all that is required to explain the observed stalactite lengths. While these analyses of the generator and stalactite mechanisms by no means prove that intense vertical drafts do not exist, they do provide a rational interpretation of the radar observations and of light turbulence observed from aircraft flying near the bases or tops of altostratus layers.

This study of the stalactite mechanism has been extended by consideration of the instantaneous evaporation case as it applies along the special lines $x=0$ and $x=L/2$, where there is no horizontal advection. The simple equations that facilitate solution along these verticals are based on an extension of reasoning discussed in sections 1 and 2. Consider first the case of instantly evaporating precipitation falling into an unsaturated updraft. The air above the level to which the leading edge of precipitation has descended is saturated and condensation therein causes the growth of precipitation above that leading edge. The vertical distribution of precipitation in the updraft *above the precipitation base* is, therefore, the same as that previously computed in the one-dimensional updraft case except for the additive constant in equation (3), $M(H)$, the precipitation water content at the upper cell boundary. Equation (3) also defines condensate distributions in the saturated descending air overtaken by precipitation falling along the line $x=0$. The time between the initial state and the final steady state in a small height interval can be calculated from the steady-state final condition, the initial condition, and the wind field. The equation used to determine the time elapsed is a finite-difference formulation of equation (1) for the one-dimensional incompressible case, viz.,

$$\frac{M_{z,f}-M_{z,i}}{\Delta t}=-w_z\left[\frac{M_{z+\Delta z,f}-M_{z-\Delta z,i}}{2\Delta z}-G_z\right]-\frac{(VM)_{z+\Delta z,f}-(VM)_{z-\Delta z,i}}{2\Delta z} \tag{28}$$

The distributions of all quantities in equation (28) except $\Delta t$ are specified, and it is therefore simple to solve for $\Delta t$. Equation (28) has been solved for $\Delta t$ in five different vertical air currents where the initial moisture distribution is defined by $M_i=(-2+z/H)$ gm./m.$^3$, $G=10^{-3}$ gm./m.$^4$, and $H=10^3$m. The results are illustrated in figure 13, where it is seen that the particular

assumptions regarding the rate of addition of moisture at $z=H$ and the initial dryness of the air lead to a balance between the vertical advection of dry air and the descent of condensate in the updraft cases. In these updraft cases, therefore, stalactite lengths as measured by the difference in height of the precipitation base at $x=0$ and $x=L/2$ would be indefinitely long. Of course, the cell that gives rise to the stalactite phenomenon does not have an indefinitely persisting circulation. If it did, it would eventually become saturated throughout by a return flow of vapor from its downdraft portion and the portion of the cell in which precipitation is held aloft would become indefinitely smaller with time. Circulations actually decay before such limits are reached.

The foregoing leads to another interesting consideration. The steady precipitation emerging beneath the updrafts of a convective cell imbedded in a saturated atmosphere has a higher intensity, and that emerging from the downdraft side has, due to evaporation in saturated downdrafts, a smaller intensity than the precipitation entering the cell at the top. This indicates how, in a vertical air circulation, stratiform precipitation falling through the circulation is redistributed and emerges with horizontal gradients of intensity. The distributions for a saturated atmosphere are easily computed, and may be useful in interpreting radar records where small convective cells are established within widespread precipitation by microphysical effects, as is often the case, for example, near the level where snow melts to rain (Wexler [16] and Newell [11]).

## 8. CONCLUSIONS

The continuity equations are powerful tools for illuminating fundamental properties of wind-water relationships. The greatest advances should come as theory and observation are combined, so that each supplements and complements and indicates paths of useful development for the other. Application of kinematic theory to analyses of conventional data with satellite photographs and distributions of radar reflectivity and Doppler velocity should yield improved descriptions of the wind field accompanying precipitation and of the associations of these fields with wind shear, static stability, and other quantities of dynamical significance.

It is important to generalize the theory to account for and evaluate the bulk effects of cloud physics processes. This avenue of study is relevant to the problems of weather modification by such means as artificial seeding. A preliminary discussion of such a generalization is contained in Kessler and Newburg [7].

As dynamical numerical models of the atmosphere become more sophisticated, equations of continuity for cloud and precipitation in more nearly natural forms will be incorporated therein and should reveal how the air motions, water transports, and cloud physics processes interact to determine the scales, shapes, and intensities of convective events. The recent works by Lilly [8], Malkus and Witt [9], Ogura and Phillips [12], Saltzman [13], and Sasaki [14], for example, may provide suitable thermohydrodynamic frameworks for such advanced studies.

## ACKNOWLEDGMENTS

The manuscript was reviewed by Dr. Edward Newburg and Mr. George Kern, of TRC, who also contributed via several stimulating discussions. Mr. Albert Chmela, of the Weather Radar Branch, Air Force Cambridge Research Laboratories, determined the solutions illustrated in the lower row of figure 4, and Mr. Paul Duchow, of The Travelers Research Center, Inc., computed those shown in the lower row of figure 5. Mr. Rudolf Loeser, of AFCRL, and Mr. Brian Sackett, of TRC, drafted the figures.

## REFERENCES

1. D. Atlas, "The Radar Measurement of Precipitation Growth," Sc. D. Thesis, Massachusetts Institute of Technology, 1955, (See Appendix).
2. R. H. Douglas, K. L. S. Gunn, and J. S. Marshall, "Pattern in the Vertical of Snow Generation," *Journal of Meteorology*, vol. 14, No. 2, Apr. 1957, pp. 95–114.
3. E. Kessler, III, "Radar-Synoptic Analysis of an Intense Winter Storm," *Geophysical Research Papers*, No. 56, U.S. Air Force Cambridge Research Center, Oct. 1957, 218 pp.
4. E. Kessler, III, "Kinematical Relations Between Wind and Precipitation Distributions," *Journal of Meteorology*, vol. 16, No. 6, Dec. 1959, pp. 630–637.
5. E. Kessler, III, "Kinematical Relations Between Wind and Precipitation Distributions, II," *Journal of Meteorology*, vol. 18, No. 4, Aug. 1961, pp. 510–525.
6. E. Kessler, III and D. Atlas, "Model Precipitation Distributions," *Aero/Space Engineering*, vol. 18. No. 12, Dec. 1959, pp. 36–40.
7. E. Kessler, III and E. Newburg, "Relationships between Tropical Precipitation and Kinematic Cloud Models," First Quarterly Progress Report on Signal Corps Contract DA 36–039 sc 89099, Travelers Research Center, Inc., 1962.
8. D. K. Lilly, "On the Numerical Simulation of Bouyant Convection," *Tellus*, vol. 14, No. 2, May 1962, pp. 148–172.
9. J. S. Malkus and G. Witt, "The Evolution of a Convective Element; A Numerical Calculation," in *The Atmosphere and the Sea in Motion*, Rockefeller Institute Press, New York, 1959, pp. 425–439.
10. J. S. Marshall, "Precipitation Trajectories and Patterns," *Journal of Meteorology*, vol. 10, No. 1, Feb. 1953, pp. 25–29.
11. R. Newell, "Some Radar Observations of Tropospheric Cellular Convection," *Research Report* No. 33 by Weather Radar Research, Massachusetts Institute of Technology, on Contract AF 19(604)–2291, 1959.
12. Y. Ogura and N. A. Phillips, "Scale Analysis of Deep and Shallow Convection in the Atmosphere," *Journal of the Atmospheric Sciences*, vol. 19, No. 2, Mar. 1962, pp. 173–179.
13. B. Saltzman, "Finite Amplitude Free Convection as an Initial Value Problem, I," *Journal of the Atmospheric Sciences*, vol. 19, No. 4, July 1962, pp. 329–341.
14. Y. Sasaki, "Effects of Condensation, Evaporation and Rainfall on the Development of Mesoscale Disturbances: A Numerical Experiment," *Scientific Report No. 1*, Texas A. and M. College on Contract AF 19(604)–6136, 1960.
15. A. F. Spilhaus, "Raindrop Size, Shape and Falling Speed," *Journal of Meteorology*, vol. 5, No. 3, June 1948, pp. 108–110.
16. R. Wexler, "Advection and the Melting Layer," *Meteorological Radar Studies* No. 4, Blue Hill Meteorological Observatory, Harvard University, Contract AF 19(604)–950, 1957, 12 pp.